ISBN: 978-3-95450-184-7 doi:10.18429/JACoW-IPAC2018-THPAL085

HIGH POWER RF CONDITIONING ON CLARA

L.S. Cowie[1], D. Scott, STFC Daresbury Laboratory, Warrington, UK
G. Burt, W.L. Millar, Lancaster University, Lancaster, UK
[1]also at Lancaster University, Lancaster, UK

Abstract

The CLARA accelerator at Daresbury Laboratory will have 8 normal conducting RF cavities. Automating the high power RF conditioning of these cavities will mean a repeatable, research-lead process is followed. An automated algorithm has been written in Python. A prototype algorithm was used to condition the first CLARA travelling wave linac in October 2017. The linac was successfully conditioned over approximately 12 million pulses up to 27 MW for a 750 ns pulse. A more complex and robust algorithm was used to re-condition the standing wave 10 Hz photoinjector after a cathode change. The photoinjector was conditioned to 10 MW for a 2.5 μs pulse in February 2018 over 2.1 million pulses. Conditioning method; differences for travelling and standing wave structures; difficulties and interesting phenomena are all discussed.

INTRODUCTION

The CLARA FEL at Daresbury Laboratory will operate at 250 MeV [1]. The S-band RF system will include a 120 MV/m RF photoinjector, four travelling wave linacs, two standing wave dipole mode diagnostic cavities and an X-band travelling wave lineariser.

In 2016 Wuensch et al [2] concluded from statistical data that an RF cavity conditions with the number of pulses, not the number of breakdowns. Breakdowns are well known to damage the surface of cavities and limit the gradient [3]. In light of this research it is clear that limiting the number and severity of breakdowns during conditioning is best practice, particularly for high gradient structures, like the 120 MV/m CLARA injector.

To condition in a reliable and repeatable way, the conditioning must be automated. The conditioning algorithm used on the CERN XBOX X-band test stands [4] was used as a basis for a python program. The RF power is ramped at a constant rate subject to an allowable breakdown rate. On detection of a breakdown the RF power is turned off briefly to avoid follow up breakdowns [5].

Breakdowns can be detected through the RF signals, the dark current level, and the vacuum pressure.

LINAC 1 CONDITIONING

The conditioning of the first linac on CLARA at Daresbury Laboratory was completed in October 2017. The linac is a 2 m 2.9985 GHz travelling wave structure designed and fabricated by Research Industries GmBh. The conditioning was performed by a prototype python program, which ramped the RF at a constant rate regardless of breakdown rate, and detected breakdowns when spikes were seen in the reflected power and the vacuum pressure. This was performed in steps of 0.25 μs pulse length.

The linac was conditioned over approximately 12 million pulses up to 27 MW for a 750 ns pulse at 50 Hz. The rolling breakdown rate was approximately 3×10^{-5} breakdowns per pulse. The cavity achieved a gradient of 21.5 MV/m and successfully accelerated electron beam.

The cavity conditioned smoothly, although recurring arcing in the klystron protection circulator occasioned a disruption in the conditioning whist cleaning was performed. The conditioning was completed in two discrete periods.

Saving RF traces on breakdown commenced part way through the first conditioning period after 6 million pulses. The cavity forward and reflected power were measured at a directional coupler above the vacuum window, and the power was also saved from the probe in cell 57.

The breakdowns can be categorised as structure arcs or vacuum events. Some RF traces that were classed as breakdowns show no pulse, and some show a very low (~0.5%) forward and reflected pulse, both of which are unexplained. There was a high incidence of false alarms where normal pulses were miscategorised as breakdowns, as the breakdown detection was tested at high power for the first time. The number of occurrences of each of the categorised events is shown in Table 1.

Table 1: Breakdown Events by Type and Location

Event	Period 1	Period 2	Total
All	680	699	1379
No data saved	473	0	473
Vacuum Spike	45	31	76
Structure Arc	129	60	189
False Alarm	32	359	391
No Pulse	30	122	152
Low Power Pulse	14	84	98

The edge method [6] was used to determine the location of the structure arcs. The RF power at the output coupler is usually used in this method, but this was not saved, so the method was modified to use the power measured at the probe in cell 57, as such all breakdowns after this point have been averaged over the remaining 3 cells and the output coupler.

The cell by cell breakdown locations can be seen in Figure 1, with light blue for period 1 and darker blue for period 2. There were no particular hot cells. As the cavity is constant power dissipation rather than constant impedance or gradient the accelerating field E_{acc} increases along the structure. It can be seen in Figure 1 that the data loosely follows the breakdown rate scaling law $BDR = {E_{acc}}^{30}$[7], but the low resolution of the data means no definitive conclusion can be made.

ISBN: 978-3-95450-184-7 doi:10.18429/JACoW-IPAC2018-THPAL085

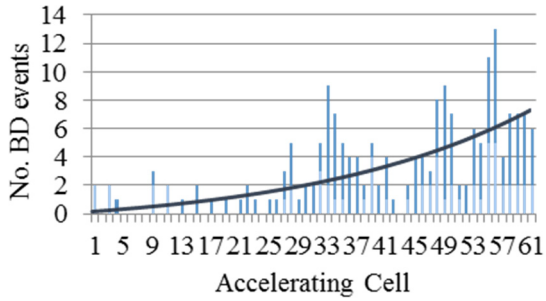

Figure 1: Breakdowns per cell where cells 1 and 61 are the input and output couplers. Cavity E_{acc}[30] in dark blue.

10 Hz INJECTOR CONDITIONING

The conditioning program was completely re-written with the new 1.5 cell 400 Hz 120 MV/m photoinjector in mind, but the aim was to be configurable for any RF structure on CLARA. The aim was a program that could, at 100 Hz, detect a breakdown and switch the RF off before next pulse. The program only allows ramping when the breakdown rate is below a set level.

The new program communicates with the EPICS control system via a C++ application programming interface, and has data-logging of machine parameters as well as all RF trace data saving upon breakdown detection.

The 10 Hz RF photoinjector is a 2.5 cell S-band gun, with a lower cathode field than the 400 Hz photoinjector [8]. The cavity is surrounded by a solenoid. It has been in operation on VELA and CLARA for 6 years. The 10 cm copper cathode backplane was replaced, so re-conditioning was required. This was used as a beta-test for the new conditioning program.

For standing wave structures the breakdown detection via RF signals must be modified from the traveling wave case due to the reflected power behaviour. Previously at ELI-NP this has been done by creating masks based on the average reflected RF trace and determining breakdowns when the mask is violated [9]. The phase of the reflected signal is much more sensitive to breakdowns than the power, and it does not change with power. Mask monitoring was therefore implemented on the phase of the reflected signal.

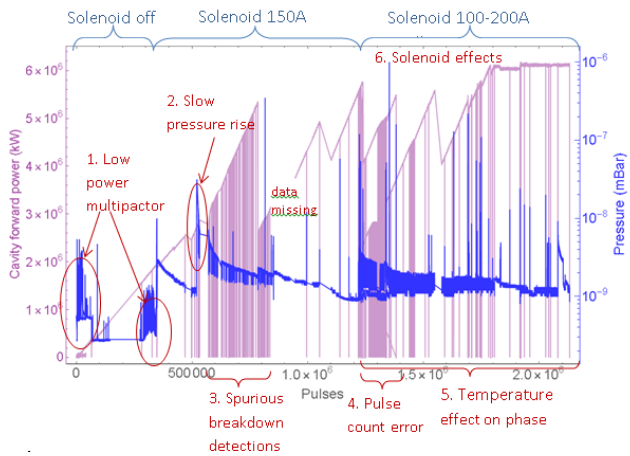

Figure 2: The cavity forward power and vacuum over the full conditioning period.

The conditioning took approximately 2.1 million pulses over 60 active hours, pulse length started at 0.5 µs and was increased in steps of 0.5 µs to 2.5 µs. The program was improved throughout the process. Cavity forward power and vacuum are shown against number of pulses in Figure 2, and the areas of interest marked, as well as the gun solenoid state. These areas of interest are discussed below.

Breakdowns

An exemplar breakdown is shown in Figure 3. The breakdown occurred at the end of the pulse.

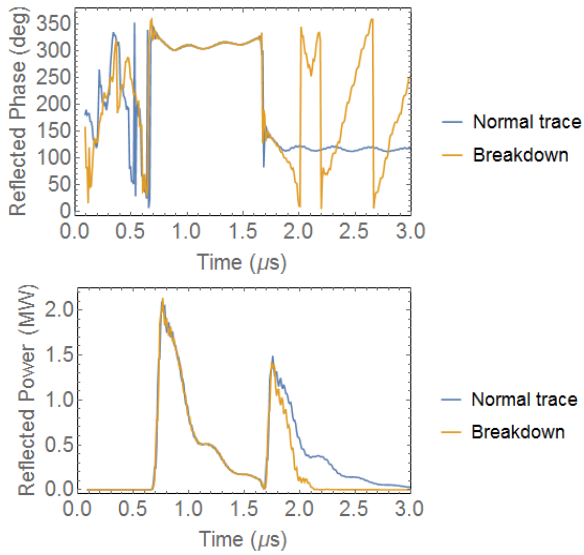

Figure 3: Reflected power and phase during breakdown.

Low power multipactor

When the peak forward power reached 80 kW at 0.5 µs pulse length, cavity activity was detected by the conditioning software, both in the cavity reflected RF phase and the vacuum. The cavity reflected power and phase during one of these events can be seen in Figure 3. It can be seen that the phase of the instantaneous reflected RF power from the cavity has a sharp rise 0.6 µs after the forward power pulse is switched off. A slight drop in instantaneous reflected power can also be seen at this point. The pressure in the cavity spiked during these events. The baseline pressure was 6 x 10^{-10} mbar, and the spikes were small, up to 2.5 x 10^{-9} mbar.

Multipactor is the obvious conclusion for this effect. It is interesting however that the multipactor occurs when the cavity is emptying, but only at specific peak forward power levels. This behaviour was seen between 80 & 150 kW, and again between 1.5 & 1.9 MW. The first band of multipactor occurs when there is approximately 5000 W instantaneous power exiting the cavity. The stored energy in the cavity must reach the same level at lower peak forward power levels, and also as the cavity is filling, but his effect is only seen at certain peak power bands and only as the cavity empties, this is most likely because the rate of change of cavity stored energy is low-

ISBN: 978-3-95450-184-7 doi:10.18429/JACoW-IPAC2018-THPAL085

est at this point in the pulse, giving multipactor time to build up (Figure 4).

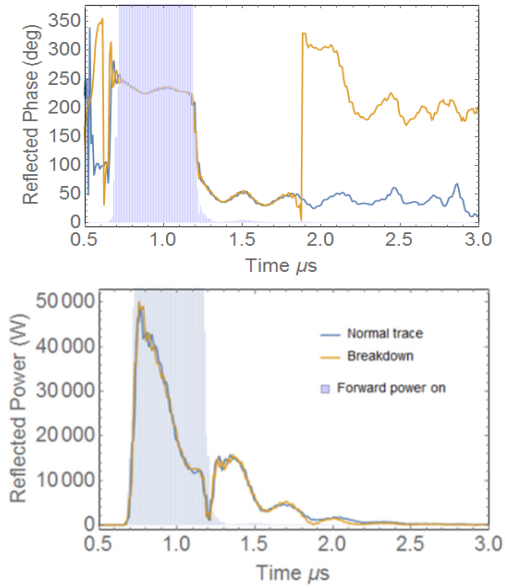

Figure 4: Reflected phase and power during multipactor.

It was decided to alter the program to ignore these very low power effects as the risk of cavity damage was low and treating these as breakdowns meant conditioning was effectively stalled. It should be noted that on returning to the lower power range later in the conditioning process no events were seen, as such it appears to be a soft multipactor barrier.

Slow pressure increase

Another low power effect that was seen on one occasion was a slow pressure increase. There were two small vacuum spikes, 6 seconds apart (5 x 10^{-9} and 7 x 10^{-9} mBar respectively) each with no change in the RF phase detected. After another 7 seconds the cavity pressure began to rise, reaching 3 x 10^{-8} mBar after approximately 3 minutes. This is quite a high pressure considering no change was seen in the RF throughout. A possible explanation is that this is neutral gas outgassing through a localised heating effect.

Spurious breakdown detections

Spurious breakdown detections occur when the acquired forward power drops to zero. This seems to be a problem with acquisition from the LLRF system. This effect got worse at around 500000 pulses when the RF trigger was switched from the RF master oscillator to the laser trigger. This can be seen in Figure 2. It was noticed that the drops were more likely to occur when the LLRF set point was changed by the python program, and a change in the method for this change within the python alleviated this problem somewhat, but not entirely.

Temperature effect on phase

At pulse lengths longer than 2 μs, the reflected phase was seen to vary towards the end of the pulse. Figure 5 shows a plot of the instantaneous reflected phase increasing over the pulse. At other times it was seen to decrease. This correlates with temperature changes in the cavity.

Up to 1°C of temperature fluctuation occurred due to the conditioning program misdiagnosing the phase changes as breakdowns and repeatedly turning the power off.

1°C of temperature change causes approximately 50 kHz frequency error in the cavity. The phase variation is caused by the phase mismatch between the power reflected by the coupler and that coming out of the coupler from the detuned cavity and is reproducible in simulation.

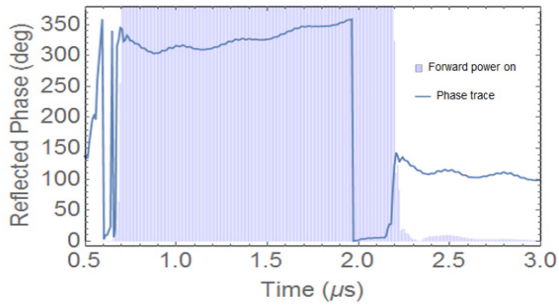

Figure 5: Reflected phase due to cavity detuning.

Solenoid Effects

Due to programme changes, the solenoid was turned on when conditioning had reached 0.5 μs pulse length with 1.9 MW peak forward cavity power. The solenoid was switched on to 150 A, as was used previously. This caused the vacuum baseline to rise from 3 x 10^{-10} to 2.7 x 10^{-9} mbar. The vacuum level then recovered slowly to around 1 x 10^{-9} mbar.

Later in the conditioning process at the solenoid was oscillated from + 100 A to + 200 A in order to give more flexibility during operation. The effect on the vacuum can be seen in Figure 6 below.

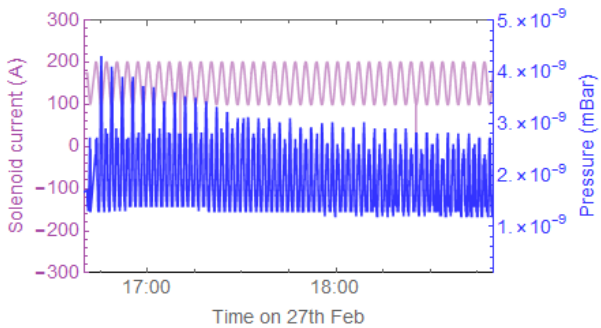

Figure 6: Effect of solenoid oscillation on cavity pressure.

CONCLUSION

Work is continuing at Daresbury Laboratory on applying new research to conditioning procedures and employing higher levels of automation. The next structure to condition is the 120 MV/m 400 Hz photoinjector, which will benefit from the lessons learned on the structures presented here.

REFERENCES

[1] J. A. Clarke *et al.*, "CLARA Conceptual Design Report", 2014 JINST 9 T05001.

ISBN: 978-3-95450-184-7 doi:10.18429/JACoW-IPAC2018-THPAL085

[2] W. Wuensch *et al.*, "Comparison of the conditioning of high gradient accelerating structures", *Phys. Rev. Accel. Beams*, vol. 19, p. 032001, Mar 2016.

[3] V. A. Dolgashev, "Experiments on gradient limits for normal conducting accelerators", in *Proc. 21st Int. Linear Accelerator Conf. (LINAC'02),* Gyeoungju, Korea, Aug. 2002.

[4] B. Wooley, "High power X-band RF test stand development and high power testing of the CLIC crab cavity", Lancaster University, Lancaster, UK, 2015, 173 p.

[5] W. Wuensch *et al.*, "Statistics of vacuum breakdown in the high-gradient and low-rate regime", *Phys. Rev. Accel. Beams*, vol. 20, p. 011007, Jan 2017.

[6] R. Rajamäki, "Vacuum arc localization in CLIC prototype radio frequency accelerating structures", Aalto University, Helsinki, Finland, 2016.

[7] S. Doebert et al. "High Gradient Performance of NLC/GLC X-band accelerating structures", in *Proc. Particle Accelerator Conf 2005. (PAC'05),* Knoxville, Tennessee, USA, May 2005.

[8] J. Rodier *et al*., "Construction of the ALPHA-X photo-injector cavity", in *Proc. 10th Eur. Particle Accelerator Conf. (EPAC'06)*, Edinburgh, UK, Jun, 2006.

[9] S. Pioli *et al*., "The real-time waveform mask interlock system for the RF gun conditioning of the ELI-NP gamma beam system", in *Proc. 8th Int. Particle Accelerator Conf. (IPAC'17)*, Copenhagen, Denmark, May, 2017.